

Research Paper

Cite this article: Pushpakaran SV, Purushothama JM, Mani M, Chandroth A, Pezholil M, Kesavath V (2018). A metamaterial absorber based high gain directional dipole antenna. *International Journal of Microwave and Wireless Technologies* **10**, 430–436. <https://doi.org/10.1017/S1759078718000454>

Received: 23 August 2017
Revised: 20 February 2018
Accepted: 21 February 2018
First published online: 3 April 2018

Keywords:

Absorbers; dipole antenna; metamaterials; reactive to propagating conversion

Author for correspondence:

Sarin Valiyaveetil Pushpakaran, E-mail: sarincrema@gmail.com

A metamaterial absorber based high gain directional dipole antenna

Sarin Valiyaveetil Pushpakaran¹, Jayakrishnan M. Purushothama², Manoj Mani², Aanandan Chandroth², Mohanan Pezholil² and Vasudevan Kesavath²

¹Department of Electronics, Government College Chittur, Palakkad, Kerala-678104, India and ²Centre for Research in Electromagnetics and Antennas, Cochin University of Science and Technology, Cochin-22, Kerala, India

Abstract

A novel idea for generating directional electromagnetic beam using a metamaterial absorber for enhancing radiation from a microwave antenna in the S-band is presented herewith. The metamaterial structure constitutes the well-known stacked dogbone doublet working in the absorption mode. The reflection property of the dogbone metamaterial absorber, for the non-propagating reactive near-field, is utilized for achieving highly enhanced and directional radiation characteristics. The metamaterial absorber converts the high-spatial reactive spectrum in the near-field into propagating low-spatial spectrum resulting in enhanced radiation efficiency and gain. The gain of a printed standard half-wave dipole is enhanced to 10 dBi from 2.3 dBi with highly directional radiation characteristics at resonance.

Introduction

Electromagnetic wave propagation through periodic guiding structures has been a constant source of inspiration for research community over the decade [1]. Even though the transmission and reflection spectra could be controlled by periodically loading inductors and capacitors in a transmission line, the invention of metamaterials has given an additional degree of freedom for controlling electromagnetic wave propagation [2]. The unusual dispersive nature of periodic metamaterial elements gives rise to different propagation scenarios like negative refractive index, near-field lensing etc [3]. In left-handed materials, phase and group velocities are anti-parallel to each other and a variety of studies has been focused on the phenomenon in microwave and THz regime [4,5].

The ability to exercise independent control over the phase and magnitude of reflection and transmission coefficients gives an interesting outlook and attraction to metamaterials in contrast to the conventional materials [6,7]. Negative refractive index property could be easily implemented using the stacked metal slab pairs [8,9]. The metal slab pairs exhibit both electric and magnetic resonances. Both these resonances can be controlled and could be merged each other yielding negative refractive index behavior. Another convenient method is to use the stacked dogbone metamaterial in which independent control of resonances could be easily achieved [10]. There is a close correspondence between the transmission characteristics of stacked perforated arrays [11] and stacked dogbone metamaterials [12].

Among the numerous applications of metamaterials, an important feature is electromagnetic absorption using engineered electric and magnetic inclusions. The basic theory behind absorption is to make equal values of electric and magnetic dipole polarizabilities on the composite [13]. In finite difference time domain (FDTD) simulations, perfectly matched layer (PML) boundary is used for electromagnetic wave absorption [14]. It is well known that an electromagnetic source generates both propagating as well as evanescent waves. Propagating plane waves are responsible for far-field radiation and the evanescent wave contains sub-wavelength information about the source and is decayed exponentially within the near-field of the excitation. PML layer absorbs energy contained in the propagating spectrum of the electromagnetic wave whereas evanescent wave undergoes reflection from the boundary [15]. Recently, Tretyakov et. al. introduced the concept of conjugately matched layer (CML) for matching the high-spatial reactive power in addition to the propagating ones [16]. Unlimited power reflection can be achieved by placing random sub-wavelength particles above the CML layer. Therefore, the interaction of evanescent and real propagating waves with matter is of great concern in metamaterial research.

An evanescent wave behaves differently with matter as compared with a real propagating wave [17]. The real part of refractive index adds phase shift for a propagating wave and the imaginary part of refractive index introduces energy dissipation in the form of absorption. For an evanescent wave, the real part of refractive index introduces absorption and the imaginary part is responsible for phase shift. Therefore, the imaginary part of refractive index causes reflection from the material sample under consideration. There is a close resemblance between

the motion of electrons under the potential function and electromagnetic wave interaction with matter [17].

In this paper, the reflection offered by the artificial dogbone metamaterial absorber is used for achieving greatly enhanced and directional radiation characteristics from a standard printed dipole antenna. The absorber converts the reactive high-spatial spectrum existing in the near-field of the antenna into propagating low-spatial ones, which greatly enhances the radiation performance of the antenna. Simulation studies are performed using CST Microwave Studio and experiments are validated using the Agilent PNAE8362B network analyzer. Radiation performance of the proposed antenna is compared with a conductor backed dipole and the effect of loading height on antenna performance are also studied.

Theory and characterization of the metamaterial

The metamaterial unit cell considered here is the stacked copper plates made in the shape of Dogbone cell etched on a low-cost epoxy substrate with dimensions as shown in Fig. 1. The epoxy substrate is characterized by a dielectric constant 4.4 with thickness 0.8 mm. The final fabricated array contains 10×10 elements with stacking height denoted by d_z . The metamaterial array is fabricated using the standard photo-lithographic etching techniques.

When a time-varying electromagnetic wave with polarization along Y-axis is applied as shown in Fig. 1, resonance can be excited on the metamaterial and the nature of resonance could be controlled by varying the stack thickness. Commercially available electromagnetic simulation tools are equipped with functionalities to perform unit cell simulations to extract reflection and transmission coefficients of the entire array. For that, perfect electric boundary condition is applied on the upper and lower faces of the unit cell, perpendicular to the Y-axis and perfect magnetic boundary is applied on the left- and right-faces of the unit cell, perpendicular to the X-axis. Waveguide ports are assigned on

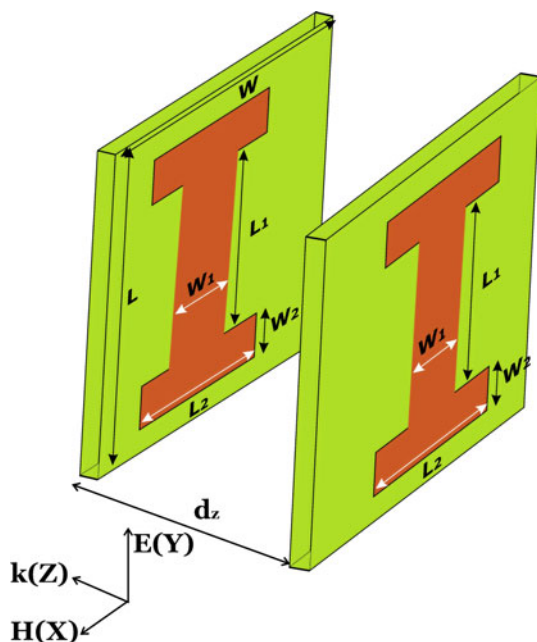


Fig. 1. Unit cell of the dogbone doublet metamaterial slab ($L_1 = 18$ mm, $L_2 = 12$ mm, $W_1 = 4$ mm, $W_2 = 2$ mm, $L = W = 24$ mm).

the air extended front and back faces of the unit cell with electric field orientation along Y-axis. This will allow the propagation of transverse electromagnetic waves along Z-direction with polarization along Y-axis.

The variation in reflection, transmission, and absorbance of the structure with stacking height d_z is given in Fig. 2. It is evident that increase in stacking thickness enhances the transmission coefficient at resonance for normal incidence. For $d_z = 1$ mm, the low values of reflection and transmission coefficients at resonance (3.1 GHz) indicate that the metamaterial structure is acting as an electromagnetic absorber. This case gives maximum absorption and the absorbance is found to be nearly 80% at resonance. The absorbance (A) of the structure has been calculated from the transmittance (T) and reflectance (R) using the relation, $A(\omega) = 1 - T(\omega) - R(\omega)$.

The structure shows near unity resonant transmission for $d_z = 4$ mm onwards and this mode has been used for achieving left-handed transmission behavior for microwave applications [9,10,18]. Left-handed transmission peaks are associated with

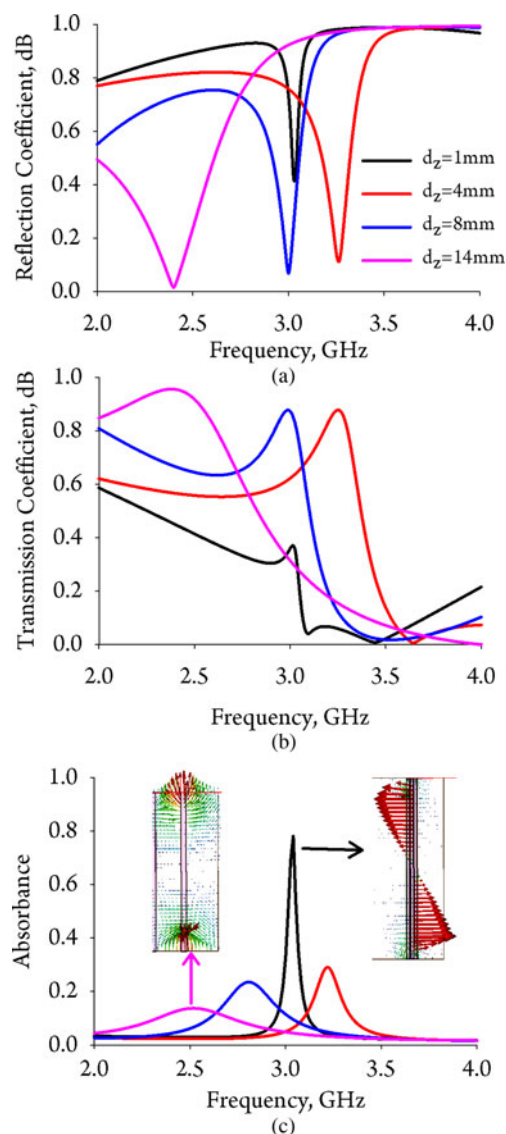


Fig. 2. Effect of stack thickness on (a) reflection, (b) transmission coefficients, and (c) absorbance with electric field distributions in the inset.

minimum absorbance as dictated in Fig. 2(c). The power transmission enhancement of cut-wire pairs finds applications in using this metasurface as a superstrate for enhancing the radiation performance of dipole antennas [18]. The side view of simulated electric field distributions on the unit cell for $d_z = 1$ mm and $d_z = 14$ mm are also shown in the inset of Fig. 2(c). It is noted that for a lower stacking height, E_z component of electric field is dominating over the E_y component. So initial increase in d_z decreases the capacitance between the plates and resonance is shifted towards the higher side. For higher stacking heights, magnetic resonance is excited and the E_y component of electric field is dominating over the E_z component. Hence, for higher stacking heights, increase in d_z lowers the resonant frequency of the metamaterial. This is due to the fact that magnetic resonance is excited due to the anti-parallel currents on the lower and upper metallic plates of the metamaterial unit cell.

The effective material parameters of the medium are extracted using the Ziolkowski method [19] and the retrieved values are depicted in Fig. 3. Since the study is focused on the absorption resonance, the parameters for $d_z = 1$ mm is considered here. It is evident that the structure shows strong permittivity resonance yielding negative values of permittivity after resonance. Since magnetic dipole resonance is absent, the structure could be identified as an artificial dielectric exhibiting negative permittivity after resonance. The positive permittivity peak before resonance can be used for superstrate applications. An increase in stacking thickness further excites magnetic response and shows left-handed transmission peaks. Further studies in this regard have been omitted for brevity. Corresponding to the electric resonance, the imaginary part of permittivity attains a huge value resulting in electromagnetic absorption for propagating waves. It is well known that increasing the value of imaginary part of permittivity enhances absorption for regular propagating waves.

Maximizing absorption is a challenging task while dealing with evanescent waves as the presence of imaginary part in permittivity scatters the evanescent spectrum of an incident wave. Consider an evanescent wave traveling from air to an artificial dielectric characterized by real and imaginary part of permittivity ($\epsilon_m = \epsilon'_m - j\epsilon''_m$). The Poynting vector on the artificial dielectric medium is given by [17],

$$\langle S \rangle = [\epsilon'_m k_x, 0, \epsilon''_m k'_z] \frac{c^2}{8\pi\omega|\epsilon_m|^2} |T|^2 H_0^2 e^{-2k'_z} e^{-2zk'_z}, \quad (1)$$

where T is the Fresnel transmission coefficient, H_0 is the magnetic field of the incident beam, K_x is the transverse wave number,

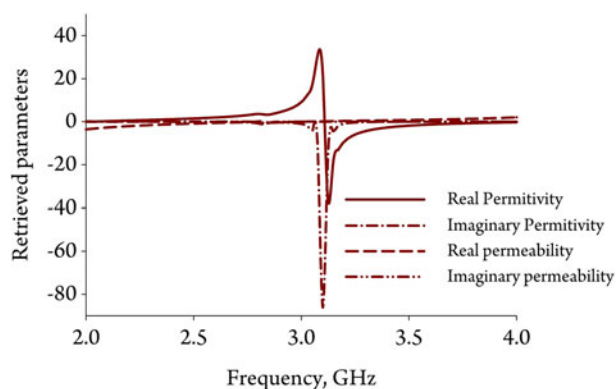


Fig. 3. Retrieved material parameters for $d_z = 1$ mm.

K_z is the longitudinal wave number and, ω is the angular frequency. For a reactive near-field, transverse oscillations would be dominant and hence, absorption can be maximized when the imaginary part of permittivity becomes zero. Increasing the value of imaginary part of permittivity decreases absorption and enhances reflection. It is also noted that reactive electromagnetic waves incident on a metal at optical frequencies gives anomalous reflection [20], in which the magnitude of reflection coefficient is greater than unity. We are experimentally showing that the anomalous reflection is due to the reactive to propagating wave conversion offered by the artificial dielectric. In this paper, the spectral conversion offered by the dogbone metamaterial absorber is utilized for enhancing the radiation performance of a microwave antenna. As per the theory, when the dogbone metamaterial absorber is placed in the vicinity of the dipole antenna, it will naturally absorb the propagating spectrum and reflects the high-spatial frequency spectrum impinging on the surface. The reflection is associated with the corresponding propagating wave conversion resulting in enhanced radiation performance.

Practical realization

For practical realization of the above concept, we have used a planar half-wave dipole antenna printed on an epoxy substrate with dimensions $L_d \times W_d$. The antenna is fed using a microstrip to slot line transition in order to avoid back currents on the feed cable of the network analyzer.

The geometrical parameters of the antennas are given in Fig. 4. The configuration of free-standing printed dipole is shown in Fig. 4(a). A Sub Miniature version-A connector is used for feeding the microstrip part of the balun structure. The dipole antenna is loaded at a height of $h_1 = 14$ mm ($0.15\lambda_0$) above the dogbone metamaterial absorber layer as shown in the side view as Fig. 4 (b). For practical realization, the antenna element is supported using a perspex holder. The metamaterial absorber array occupies an overall area of $206(2.14\lambda_0) \times 160(1.66\lambda_0)$ mm².

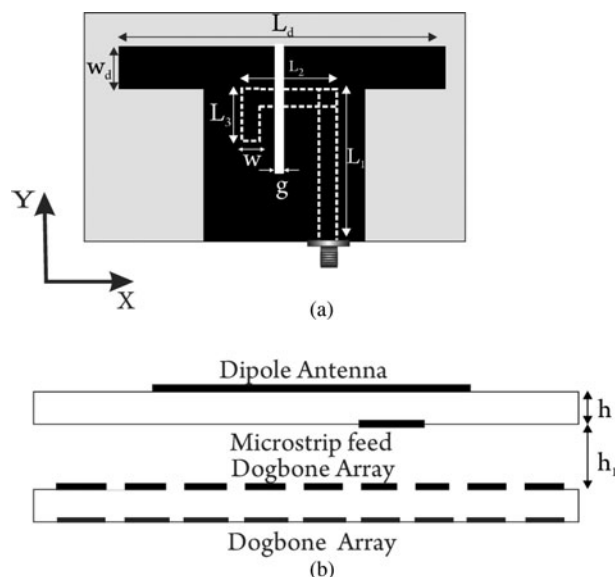


Fig. 4. Geometry of the artificial dielectric backed dipole antenna (a) Dimensions of the dipole used and (b) side view of the final antenna ($L_d = 36.5$ mm, $W_d = 5$ mm, $L_1 = 18$ mm, $L_2 = 10$ mm, $L_3 = 8$ mm, $w = 3$ mm, $h_1 = 14$ mm, $h = 0.8$ mm, and $g = 0.5$ mm).

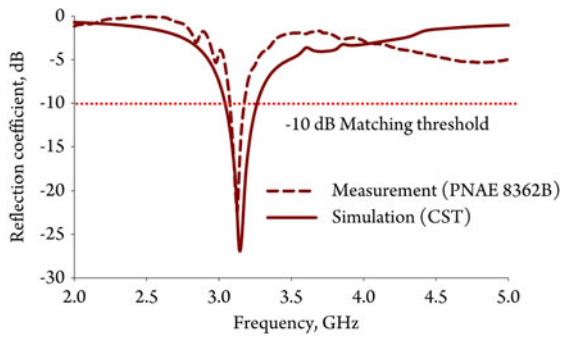


Fig. 5. Magnitude of reflection coefficient of the antenna ($h_1 = 14$ mm).

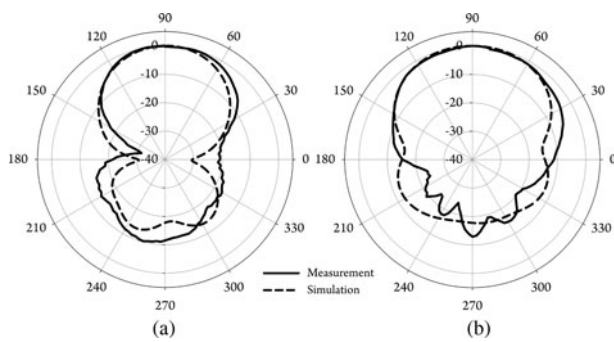


Fig. 6. Measured and simulated radiation patterns of the antenna (a) *E*-plane pattern and (b) *H*-plane pattern.

The simulated and measured reflection characteristics of the proposed absorber backed dipole antenna are shown in Fig. 5. The simulation and measurement are in good agreement with each other. The resonant frequency of the antenna is found to be 3.12 GHz with a reflection coefficient of -23 dB at resonance. The 2:1 voltage standing wave ratio (VSWR) bandwidth of the proposed design is 3.52% around resonance whereas the free-standing dipole shows an improved bandwidth of 16% at resonance. The red dotted line indicates the commonly used -10 dB impedance matching threshold level.

Far-field measurements are recorded in an anechoic chamber using an ultra wide band horn antenna. The distance between the metamaterial loaded antenna and the horn antenna is fixed as 4 m. Maximum power received from the antenna under test is noted in the boresight direction and a THRU calibration is made for normalization of the radiated power. The antenna is rotated using a computer controlled turn table assembly and the received power is recorded for the two principal planes. The measured and simulated normalized radiation patterns of the antenna in the two principal planes are shown in Fig. 6. The small discrepancies are accounted due to the measurement tolerance. The measurements confirm the directional radiation characteristics of the metamaterial loaded design. The 3 dB beam width is found to be 72° for the *E*-plane and 93° for the *H*-plane. Cross-polar isolation is found to be -25 dB for the *H*-plane pattern and -18 dB for the *E*-plane pattern. The design exhibits a front to back ratio of -12 dB at resonance. The gain of the antennas is measured using the standard gain comparison method. In the measurement, the loaded dipole shows more than three-fold increase in gain from 2.3 dBi to 10 dBi, in comparison with the unloaded free-standing case. Wheeler-Cap method has been used for the measurement of

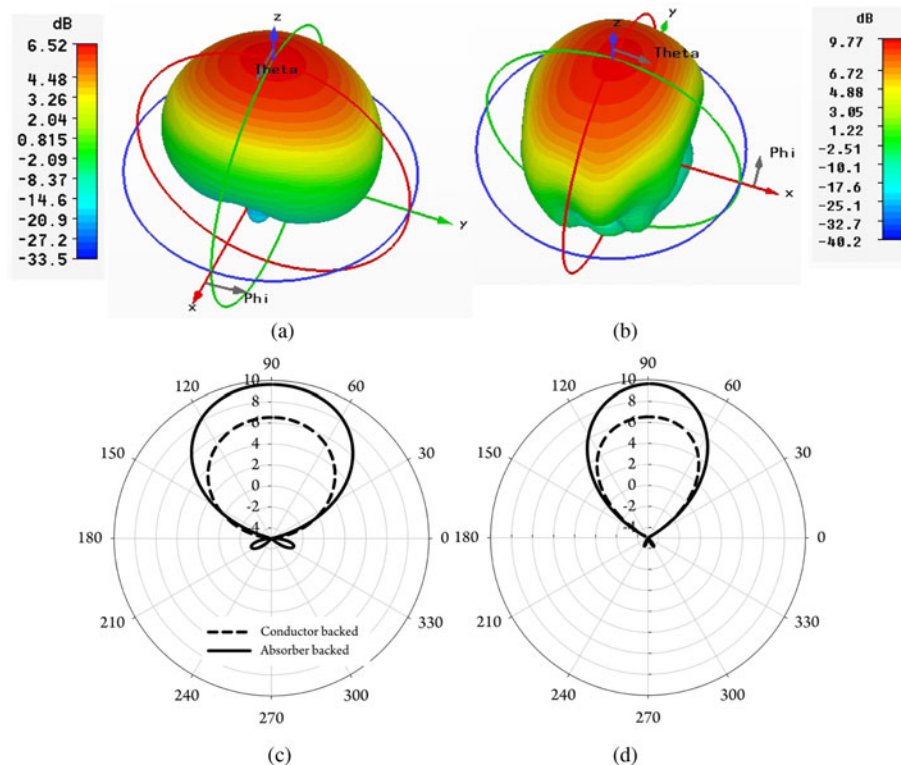


Fig. 7. Comparison of gain patterns of a conductor backed dipole and the absorber backed dipole (a) 3D gain pattern of conductor backed dipole antenna, (b) 3D gain pattern of metamaterial backed dipole, (c) comparison of *H*-plane patterns and (d) comparison of *E*-plane patterns.

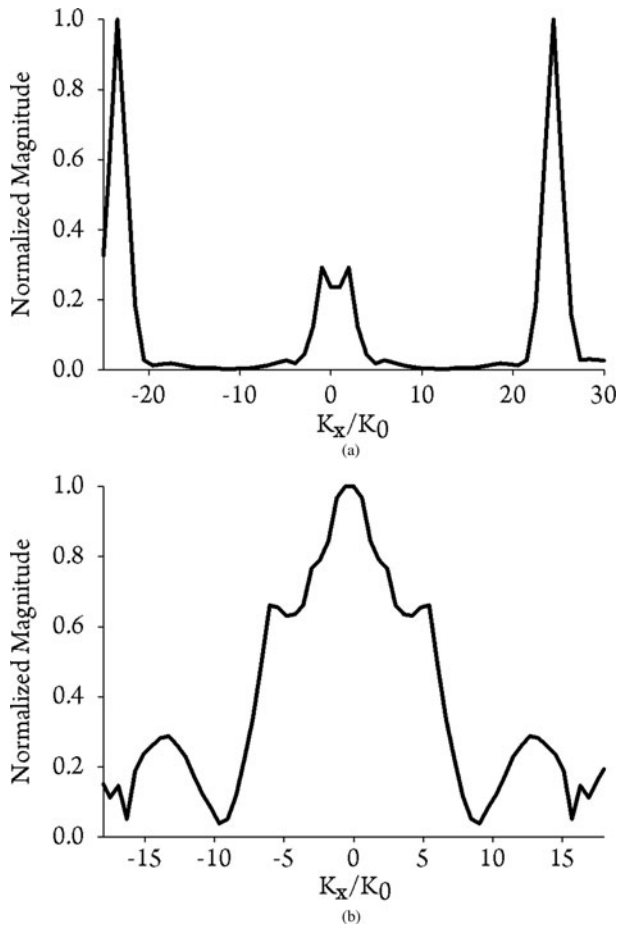


Fig. 8. Computed spatial frequency spectrum (a) free-standing dipole antenna and (b) metamaterial backed dipole antenna.

radiation efficiency of the antennas. It is found that the free-standing balun loaded dipole shows an efficiency of 85% at resonance, whereas the absorber backed design shows an enhanced efficiency of the order of 98% due to spectral conversion.

A comparison study have been performed between the radiation performance of a conductor-backed dipole antenna and the metamaterial absorber-backed dipole configuration and the results are illustrated in Fig. 7. The metal plate on the back side of the antenna occupies the same area as that of the aperture area of the metamaterial absorber and the loading heights remains the same ($h_1 = 14$ mm). Figures 7(a) and 7(b) illustrates the 3D radiated gain patterns of the two configurations. The conductor backed dipole shows a gain of only 6.3 dBi along the broadside direction whereas the proposed design achieves a gain of 9.77 dBi at resonance. Figures 7(c) and 7(d) represent the comparison between H -plane and E -plane gain patterns of the two prototypes. It can be clearly seen that the absorber backed configuration significantly enhances radiation along the upper hemisphere proving its superior performance over conductor backed designs.

The theory behind gain enhancement can be easily understood by looking into the antenna near-field. The near-field contains some useful information about the radiation behavior of the antenna. It is well known that a dipole antenna contains both propagating as well as reactive fields within its near-field. The presence of both these components can be detected by taking

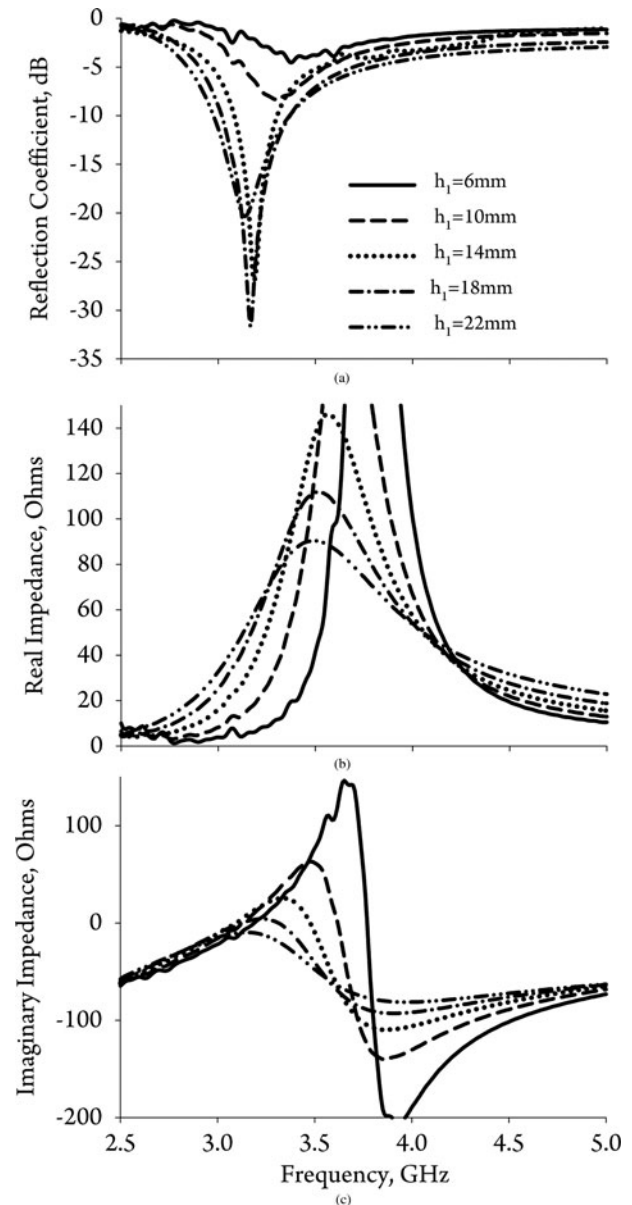


Fig. 9. Effect of loading height h_1 on antenna performance (a) variation in reflection coefficient, (b) variation real part of port impedance, and (c) variation imaginary part of port impedance.

the spatial Fourier Transform of the near-field electric field [21]. With the simulation software, it is easy to compute the electric field distributions on a plane. We have taken the spatial frequency distributions of the free-standing dipole antenna and the metamaterial absorber loaded dipole. The results are summarized in Fig. 8. Figure 8(a) shows the spatial frequency distribution of the simple dipole (without metamaterial). It is clear that the magnitude of the low-spatial frequency components corresponding to the propagating wave is comparatively low. The visible region is denoted with a region in which the ratio $|K_x/K_0| < 1$ and all other regions denote the invisible region. Invisible region contains reactive power and the visible region is responsible for far-field radiation. In the invisible region, there exists temporal phase difference between the electric and magnetic fields. The near-field of the dipole is dominated by the high-spatial frequency components designated as the reactive near-field. The presence of

the dominant reactive distributions severely affects the radiation performance of the antenna [22]. In our configuration, the meta-material absorber in effect reflects the reactive power from the antenna and converts it into low spatial propagating components. In physical sense, this is equivalent to reducing the temporal phase difference electric and magnetic fields within the near-field of the antenna. Periodic perturbations in the near-field of the source is responsible for this conversion. In the case of an optical microscope, in order to achieve super resolution, periodic perturbations in the form of dielectric cylinders are introduced resulting in spectral conversion [23, 24]. In the case of absorber loaded design, spatial conversion occurred has been verified by checking the spatial-frequency spectrum as shown in Fig. 8(b). It is clear that placing the absorber in the vicinity of the dipole converts the reactive high-spatial frequency components into low spatial propagating components. The magnitude of propagating components is found to be greatly enhanced in comparison with the free-standing dipole.

Optimum loading height h_1 is selected after running a rigorous parametric analysis in CST Microwave Studio. The effect of variation in loading height on the reflection coefficient and input impedance characteristics are illustrated in Fig. 9. It is observed that when the dipole antenna is placed in close proximity with the absorber layer, the impedance matching performance is found to be deteriorated due to highly inductive reactance. Increasing the value of h_1 improves the impedance matching performance of the antenna and it is seen that increase in loading height severely decreases the imaginary part of port impedance thereby achieving resonant matching. It is also observed that increasing h_1 increases the 2:1 VSWR bandwidth of the antenna. The higher the loading height, the higher will be the bandwidth. For the three well-matched cases ($h_1 = 14$ mm, $h_1 = 18$ mm and $h_1 = 22$ mm), the gain and radiation efficiency remains almost constant and hence $h_1 = 14$ mm has been selected as the optimum design.

Conclusions

A dogbone metamaterial-based electromagnetic absorber is utilized for enhancing the radiation performance of a standard metal plate dipole antenna working in the S-band. The anomalous reflection of reactive high spatial near-field components from an artificial dielectric exhibiting strong imaginary part of permittivity is the cause of radiation enhancement. It is observed that the reactive near-field spectrum is converted into low spatial propagating spectrum above the antenna plane. The antenna attains highly collimated radiation patterns and the gain is enhanced to 10 dBi at resonance.

Acknowledgments. The authors acknowledge the financial support received from Department of Science and Technology (DST) and University Grants Commission (UGC), Government of India.

References

1. Harvey AF (1960) Periodic and Guiding structures at microwave frequencies. *IRE Transactions on Microwave Theory and Techniques* **1**, 30–61.
2. Alu A, Engheta N, Erentok A and Ziolkowski RW (2007) Single-Negative Double-Negative and low-index metamaterials and their electromagnetic applications. *IEEE Antennas and Propagation Magazine* **49**, 23–35.
3. Engheta N and Ziolkowski R (2006) *Metamaterials: Physics and Engineering Explorations*. New York: Wiley-IEEE Press.

4. Monticone F, Estakhri NM and Alu A (2013) Full control of nanoscale optical transmission with a composite metascreen. *Physical Review Letters* **110**, 203903.
5. Pendry JB (2000) Negative refraction makes a perfect lens. *Physical Review Letters* **85**, 0–3.
6. Zhu BO, Zhao J and Feng Y (2013) Active impedance metasurface with full 3600 reflection phase tuning. *Nature Scientific Reports* **49**, 1–6.
7. Zhu BO, Chen K, Jia N, Sun L, Zhao J, Jiang T and Feng Y (2014) Dynamic control of electromagnetic wave propagation with the equivalent principle inspired tunable metasurface. *Nature Scientific Reports* **4**, 1–7.
8. Zhou J, Zhang L, Tuttle G, Koschny T and Soukoulis CM (2006) Negative index materials using simple short wire pairs. *Physical Review B* **73**, 041101.
9. Donzelli G, Vallecchi A, Capolino F and Schuchinsky A (2009) Metamaterial made of paired planar conductors: Particle resonances phenomena and properties. *Metamaterials, Elsevier* **3**, 10–27.
10. Capolino F (2009) *Metamaterials Handbook-Theory and Phenomena of Metamaterials*. Boca Raton, CA: CRC Press, Taylor and Francis Group.
11. Beruete M, Rodriguez-Ulibarri P, Pacheco-Pena V, Navarro-Cia M and Serebryannikov AE (2013) Frozen mode from hybridized extraordinary transmission and Fabry-Perot resonances. *Physical Review B* **205128**, 1–9.
12. Sarin VP, Pradeep A, Jayakrishnan MP, Chandroth A, Mohanan P and Kesavath V (2016) Tailoring the spectral response of a dogbone doublet metamaterial. *Microwave and Optical Technology Letters* **58**, 1347–1353.
13. Ra Y, Member S, Asadchy VS and Tretyakov SA (2013) Total absorption of electromagnetic waves in ultimately Thin Layers. *IEEE Transactions on Antennas and Propagation* **61**, 4606–4614.
14. Sullivan DM (2013) *Electromagnetic simulations using the FDTD method*. Piscataway, NJ: Wiley-IEEE Press.
15. De Moerloose J and Stuchly MA (1995) Behavior of Berenger's ABC for evanescent waves. *IEEE Microwave And Guided Wave Letters* **5**, 344–346.
16. Valagiannopoulos CA and Tretyakov SA (2016) Theoretical concepts of unlimited-power reflectors absorbers and emitters with Conjugately matched layers. *Physical Review B* **125117**, 1–13.
17. Anantha Ramakrishna S, Armour AD and Ramakrishna SA (2003) Propagating and evanescent waves in absorbing media. *American Journal of Physics* **71**, 562–567.
18. Saenz E, Ederia I, Ikonen P, Tretyakov S and Gonzalo R (2007) Power transmission enhancement by means of planar meta-surfaces. *Journal of Optics A: Pure and Applied Optics* **9**, 308–314.
19. Choi J, Kim J and Jung C (2013) Double-negative reconfigurable resonator with cross-polarised split rings. *Electronics Letters* **49**, 49–50.
20. Wang H (1997) Reflection of evanescent waves. *Revista Mexicana de Fisica* **6**, 916–925.
21. Tamura M (1990) Spatial Fourier transform method of measuring reflection coefficients at oblique incidence I: Theory and numerical examples. *The Journal of the Acoustical Society of America* **88**, 2259–2264.
22. Valagiannopoulos CA and Alu A (2015) The role of reactive energy in the radiation by a dipole antenna. *IEEE Transactions on Antennas and Propagation* **63**, 3736–3741.
23. Pawliuk P and Yedlin M (2014) Evanescent wave impedance and scattering conversion into radiation. *Applied Physics. B, Lasers and Optics* **114**, 407–413.
24. Ben-Aryeh Y (2008) Transmission enhancement by conversion of evanescent to propagating waves. *Applied Physics B Laser and Optics* **91**, 157–165.



Sarin Valiyaveetil Pushpakaran received his M.Sc degree in Applied Electronics in 2006 and Ph.D. degree in Microwave Electronics from Cochin University of Science and Technology, Kerala, India in 2012. He is currently an Assistant Professor in Department of Electronics, Government College Chittur, Palakkad, Kerala. His main research interests are Metamaterials, Wireless Power Transmission, Microwave Antennas and FDTD techniques.

Sarin Valiyaveetil Pushpakaran received his M.Sc degree in Applied Electronics in 2006 and Ph.D. degree in Microwave Electronics from Cochin University of Science and Technology, Kerala, India in 2012. He is currently an Assistant Professor in Department of Electronics, Government College Chittur, Palakkad, Kerala. His main research interests are Metamaterials, Wireless Power Transmission, Microwave Antennas and FDTD techniques.



Jayakrishnan M Purushothama received his B.Sc in Electronics from Aquinas College, Mahatma Gandhi University and M.Sc in Electronics Science in 2014 from Cochin University of Science and Technology, Kerala, India. His research interest includes microwave antennas, RFID tags and metamaterials.



Manoj Mani received his M.Sc in Electronics from Cochin University of Science and Technology, Kerala, India in 2015 and currently pursuing Ph.D. in Centre for Research in Electromagnetics and Antennas. He was awarded the Junior Research fellowship by University Grants Commission in 2014 and has been working at Cochin University of Science and Technology since 2015. His current

research interests include Electrically Small Antennas, RFID tags and antennas for Biomedical applications.



Aanandan Chandroth was born in India. He received the M.Sc. and Ph.D. degrees from Cochin University of Science and Technology (CUSAT), Cochin, India, in 1981 and 1987, respectively. Currently, he is a Professor in the Department of Electronics, CUSAT. He is the coordinator for Advanced Centre for Atmospheric Radar Research (ACARR) funded by Department of Science and Technology

(DST), Government of India. From 1997 to 1998, he worked at the Centro Studi Propagazione E Antenne. Consiglio Nazionale Delle Ricerche, Torino, Italy, under the TRIL program of the International Centre for Theoretical

Physics (ICTP). His research interests include microstrip antennas, radar cross section studies and frequency selective surfaces.



Mohanan Pezholil was born in India. He received the Ph.D. degree in microwave antennas from Cochin University of Science and Technology (CUSAT), Cochin, India, in 1985. Previously, he worked as an Engineer in the Antenna Research and Development Laboratory, Bharat Electronics, Ghaziabad, India. Currently he is an Emeritus Professor in the Department of Electronics, CUSAT. He is the co investigator

for Advanced Centre for Atmospheric Radar Research (ACARR) project funded by Department of Science and Technology (DST), Government of India. He has published more than 100 refereed journal papers and numerous conference articles. He also holds several patents in the areas of antennas and material science. His research areas include microstrip antennas, dielectric resonator antennas, superconducting microwave antennas, reduction of radar cross sections, and polarization agile antennas.



Vasudevan Kesavath was born in India. He received the M.Sc. degree in physics from Calicut University, Kerala, India and the Ph.D. degree from Cochin University, Cochin, India, in 1976 and 1982, respectively. From 1980 to 1984, he worked at St. Alberts College Ernakulam, Kerala, India. In 1985, he joined the Electronics Department of CUSAT where he is currently the Emeritus Professor. He is

the co investigator for Advanced Centre for Atmospheric Radar Research (ACARR) project funded by Department of Science and Technology (DST), Government of India. His research interests includes microstrip antennas, leaky wave antennas and radar cross section studies. Dr. Vasudevan is a Fellow of the Institution of Electronics and Telecommunication Engineers (India).